Journal of Physics: Condensed Matter

Dielectric properties of a mixed-valence $Pb_3Mn_7O_{15}$ manganese oxide

To cite this article: N V Volkov *et al* 2010 *J. Phys.: Condens. Matter* **22** 375901

J. Phys.: Condens. Matter **22** (2010) 375901 (6pp) doi:10.1088/0953-8984/22/37/375901

Dielectric properties of a mixed-valence $Pb_3Mn_7O_{15}$ manganese oxide

N V Volkov, E V Eremin, K A Sablina and N V Sapronova

L V Kirensky Institute of Physics, Russian Academy of Sciences, Siberian Branch, Krasnoyarsk 660036, Russia

E-mail: volk@iph.krasn.ru

Received 5 July 2010
Published 31 August 2010
Online at stacks.iop.org/JPhysCM/22/375901

Abstract

We investigated the low-frequency dielectric properties of a $Pb_3Mn_7O_{15}$ single crystal with manganese ions in the mixed-valence state (Mn^{3+}/Mn^{4+}). Dielectric relaxation was found in the frequency window from 20 to 100 kHz in the temperature range 110–180 K. The dielectric spectra of the crystal were analyzed using a Debye model. Estimations made within the model and analysis of resistivity data suggest that the relaxation behavior of the dielectric constant is related to polaronic charge carrier hopping. Around 250 K, charge ordering occurs in the crystal when the Mn^{3+} and Mn^{4+} ions are arranged in a specific order among the crystal sites. With a decrease in temperature, an ac electric field can induce a charge hop between the equivalent lattice sites available, related to crystal symmetry. This hopping is equivalent to the reorientation of an electric dipole that yields Debye-type behavior of the complex dielectric constant. The observed anisotropy in the behavior of the dielectric properties and resistivity can be attributed to a pronounced two-dimensional character of the crystal structure.

1. Introduction

At present, materials with a strong coupling between the magnetic and electrical subsystems attract much attention due to the rich physics originating from this feature [1]. The interest in these materials, well known as multiferroics, is provoked by their great application potential. Indeed, the magnetic control of electric polarization and the electric control of a spin state open new perspectives in the development of electronic devices such as magnetic (electric) memory controlled by electric (magnetic) fields, new types of attenuators, and filters.

Searching for the systems that would be characterized by both magnetic and electric orders and, possibly, their interrelation, we have focused on lead-based manganese oxides, in particular, a $Pb_3Mn_7O_{15}$ compound [2]. As is well known, the ferro- or antiferroelectric ordering state arises because the centers of positive charges in a crystal lattice do not coincide with those of negative charges. Pb^{2+} ions in the oxide contain a $6s^2$ lone pair of electrons [3], which strongly influence coordination; the resulting distorted lead coordination causes the occurrence of spontaneous electrically polarized states. On the other hand, the presence of paramagnetic Mn ions in the compound may cause the formation of long-range magnetic ordering; consequently, one may expect the coexistence of magnetism and ferroelectricity in the system. Moreover, a pronounced correlation between the magnetic and electrical order parameters is also not improbable in the mentioned compounds. Similarly, a $6s^2$ lone pair of electrons contained in Bi^{3+} ions plays a crucial role in the magnetoelectric properties of such bismuth-based materials as $BiFeO_3$ and $BiMnO_3$ [4].

Much interest in $Pb_3Mn_7O_{15}$ is also caused by the simultaneous presence of manganese ions in different oxidation states (Mn^{3+} and Mn^{4+}). The ordering of Mn^{3+} and Mn^{4+} cations in specific lattice sites yields charge localization that may affect the magnetic state of a crystal, similar to the case of doped perovskite-like manganites [5]. On the other hand, charge ordering under the specific conditions when the centers of ions with different valence do not coincide in a unit cell of the charge superstructure may cause spontaneous electric polarization [6]. Obviously, such ferroelectricity originating from density modulation is strongly coupled with the degrees of freedom of electrons; consequently, it can be effectively controlled, for example, by a magnetic field that determines the state of the magnetic subsystem. Thus, the mixed-valence manganese oxides can be considered promising for a variety of applications as materials with multiferroic properties.

Previously, we made some studies on the crystallographic structure, heat capacity, and magnetic properties of the $Pb_3Mn_7O_{15}$ single crystal [2, 7, 8]. The present study focuses on its dielectric properties and their possible correlation with the magnetic state. We measured $Pb_3Mn_7O_{15}$ dielectric susceptibility as a function of temperature, frequency, and magnetic field. As is known, dielectric spectra are extremely sensitive to the behavior of spontaneous polarization. Moreover, they can be used for probing even the local dipole moments of clusters with short-range ordering [9]. In addition, the dielectric constant gives us much information on the charge transport and charge ordering process in the materials.

2. Experimental details

Single crystals of $Pb_3Mn_7O_{15}$ were grown by a flux method. A sintering procedure was described in detail previously [2]. The crystallographic structure of the stoichiometric compound has a pronounced two-dimensional character and can be described well within an orthorhombic space *Pnma* group with the lattice parameters $a = 13.5513$ Å, $b = 17.1490$ Å and $c = 10.0909$ Å. The crystal symmetry was studied by high-resolution synchrotron powder diffraction in the temperature range 15–295 K [8]. Recall that until recently the structural properties of $Pb_3Mn_7O_{15}$ have been the subject of debate. Different research teams described the structure of the crystal alternately within hexagonal and orthorhombic symmetries [10–12]; only synchrotron radiation data will apparently put an end in this controversy. In the last, refined model, manganese ions enter the crystal in two oxidation states (Mn^{3+} and Mn^{4+}) in the ratio 4:3 and occupy nine crystallographically nonequivalent sites, each being coordinated by oxygen atoms in the octahedral configuration. A more detailed description of the synchrotron measurements and data obtained is given elsewhere [8]. Dielectric and transport measurements were performed on plate samples $3 \times 4 \times 0.2$ mm^3 in size. The sample surfaces coincided with either (001) or (100) planes of the crystal, which allowed independent measurement of the dielectric properties along the *a* axis and within the *b*–*c* plane.

The dielectric measurements were performed with a Precision Agilent LCR-meter, model E4980A, in the frequency range 10–100 kHz. Silver paint electrodes annealed at 150 °C were applied to the opposite surfaces of the samples. The transport measurements within the range 150–350 K were performed by a conventional dc four-probe method using a physical property measurement system (PPMS, Quantum Design, USA).

3. Results and discussion

The measurements of the complex dielectric constant $\varepsilon = \varepsilon' + i\varepsilon''$ show a pronounced anomaly in the temperature dependences within the range 110–180 K. In the dependence of the real part ε', the anomaly represents a sharp step-like drop with decreasing temperature. This drop coincides with a peak of dielectric loss ε''. Figure 1 shows the temperature dependences of the real and imaginary parts of the dielectric constant measured at three frequencies. The noticeable dielectric anomaly shifts towards higher temperatures with increasing frequency. This behavior indicates that in the system under study a characteristic relaxation process occurs, which can be attributed, for example, to an ion-jump mechanism [13] or localized hopping of an electron between lattice sites with a characteristic timescale [14]. The characteristic relaxation behavior is also observed in the frequency dependences of ε' and ε'' (figure 2). Thus, the frequency dependence of the dielectric loss reveals a peak, which shifts towards higher frequencies with increasing temperature. The inverse peak frequency corresponds to the characteristic relaxation time of the relaxation process occurring in the sample. The data presented in figures 1 and 2 were obtained with the measuring ac field parallel to the *a* axis. When the measuring field direction lies in the *b*–*c* plane of the crystal, the dependences have a similar form but the anomaly in the frequency and temperature dependences of ε' and ε'' differs in position and size from that obtained for the field directed along the *a* axis. Figure 3 shows the difference in the temperature dependences of ε' and ε'' for two different directions in the crystal. The anisotropy of the dielectric properties is also seen in the frequency dependences of ε' and ε''. Generally, the anisotropy of the dielectric response of the

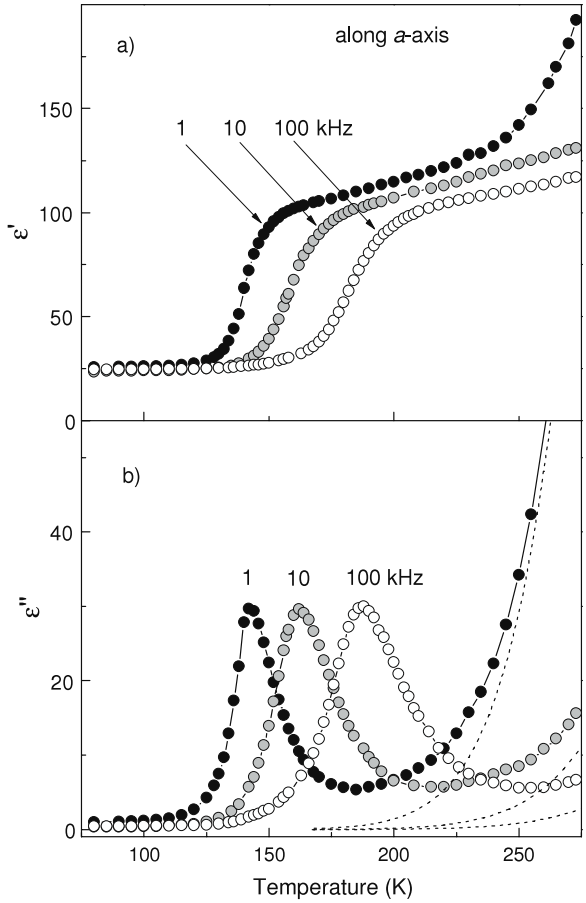

Figure 1. Temperature dependences of the real ε' (a) and imaginary ε'' (b) parts of the dielectric constant along the *a* axis; the measuring frequencies are 1, 10, and 100 kHz. The dashed lines are the temperature dependences of ε''_{dc} ($\varepsilon''_{dc} = \sigma_{dc}/(\varepsilon_0\omega)$).

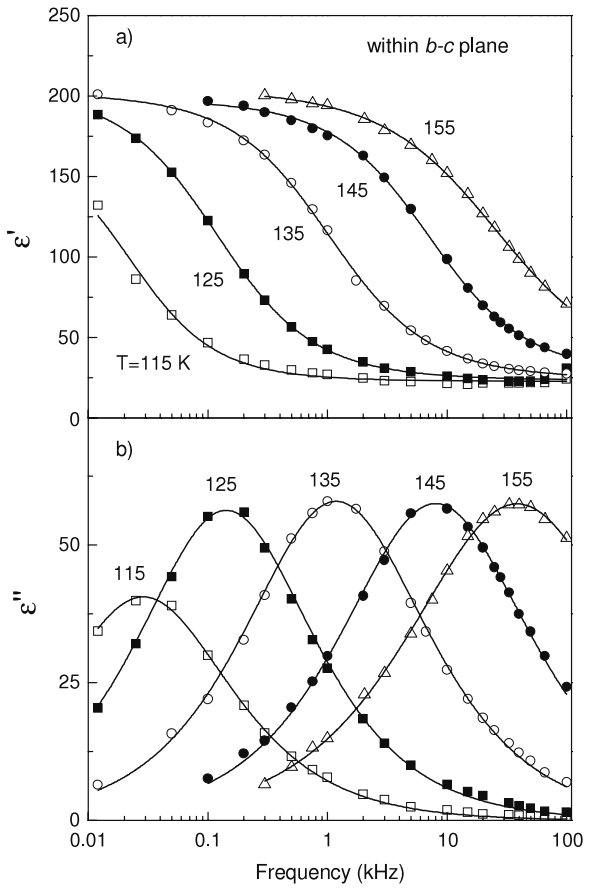

Figure 2. Frequency dependences of the real ε' (a) and imaginary ε'' (b) parts of the dielectric constant within the b–c plane for selected temperatures. The lines fit the Cole–Cole function, as described in the text.

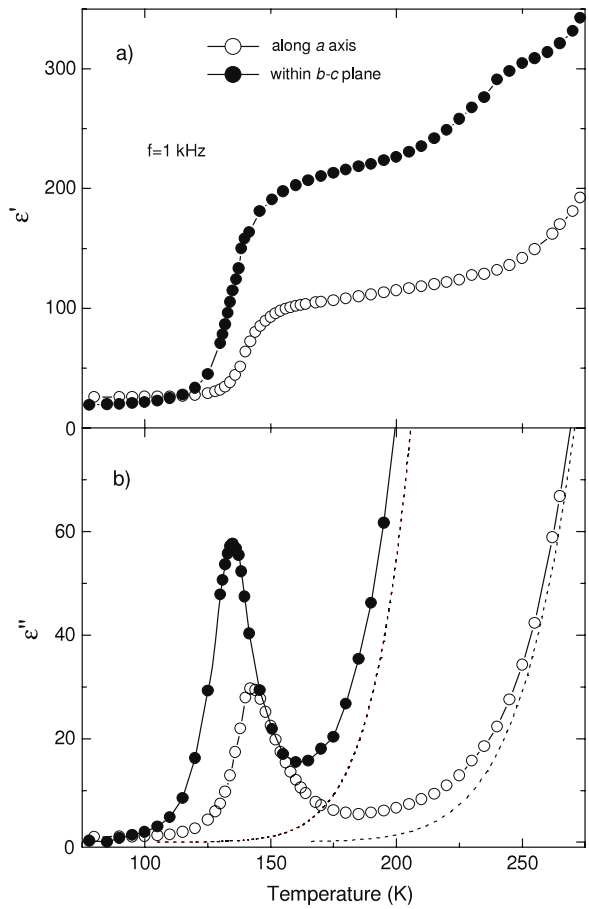

Figure 3. Temperature dependences of the real ε' (a) and imaginary ε'' (b) parts of dielectric constant at a measuring frequency of 1 kHz for two different directions in the crystal: along the a axis and within the b–c plane. The dashed lines are the temperature dependences of ε''_{dc} ($\varepsilon''_{dc} = \sigma_{dc}/(\varepsilon_0\omega)$).

$Pb_3Mn_7O_{15}$ crystal was expected from its pronounced layered structure.

Study of the dielectric properties in a magnetic field showed that at temperatures above 80 K magnetic fields up to 9 T have no noticeable effect on ε' and ε''. Yet, this does not allow definite conclusions about the direct correlation between the anomaly in the dielectric properties observed near 150 K and the feature of magnetic susceptibility that manifests itself as a broad maximum at the same temperatures [2].

Note that in the high-temperature region ε'' starts growing fast with an increase in temperature (figure 3(b)). This growth may be attributed to the increase in static conductivity of the sample σ_{dc} with temperature. The conductivity contribution to dielectric loss ε''_{dc} is determined as a ratio between σ_{dc} and frequency f at which the dielectric properties are measured: $\varepsilon''_{dc} = \sigma_{dc}/(\varepsilon_0\omega)$, where ω is the angular frequency ($\omega = 2\pi f$). The assumption is quite consistent with the character of the $\varepsilon''(T)$ dependence at different frequencies: as f grows, the dielectric loss growth in the high-temperature region slows down (figure 1). At the same time, one may conclude from figure 3 that, together with the anisotropy of the dielectric properties, $Pb_3Mn_7O_{15}$ has substantially different conductivities along different crystallographic directions. For the direction within the b–c plane, the background loss coming from dc conductivity is appreciably higher than that for the direction along the a axis. This implies higher conductivity of the crystal along the MnO_6 layers [8] (within the b–c plane) than in the direction perpendicular to them (along the a axis).

The above consideration made us perform direct measurements of conductivity for the crystal in the temperature range where the dielectric properties were measured in the two chosen directions. The temperature dependences of the dc resistivity $\rho_{dc}(T)$ both within the b–c plane and along the a axis demonstrate a semiconductor behavior; however, as we expected, there are some qualitative differences. The explicit $\varepsilon''_{dc}(T)$ dependences calculated on the basis of the experimental $\rho_{dc}(T)$ dependences are presented in figures 1 and 3. The analysis shows that the $\rho_{dc}(T)$ dependences deviate from a thermally activated behavior for both directions in the crystal; nevertheless, they are described satisfactorily under the assumption of a small polaron hopping type of conductivity. In this case, if at $T > 250$ K the temperature dependence of the resistivity follows a nearest neighboring hopping (NNH) model, then at $T < 250$K a variable range hopping (VRH) model is appropriate (figure 4). The NNH model predicts the following: $\rho_{dc}(T) = \rho_0 T \exp(E_a/k_B T)$ [15] where ρ_0 is the temperature-independent coefficient, E_a is the activation

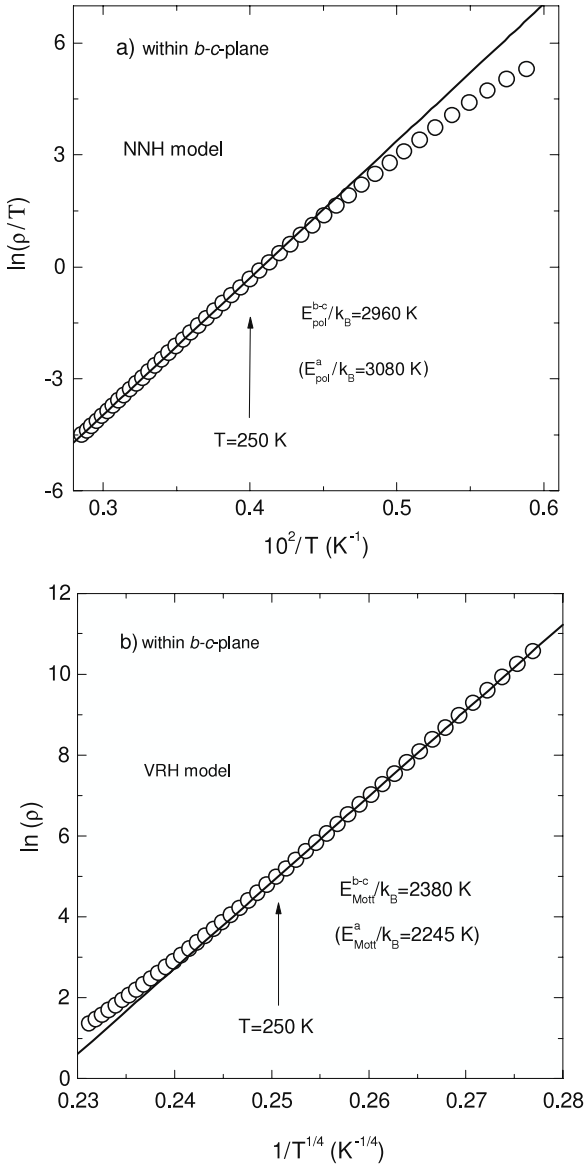

Figure 4. DC resistivity scaled to the NNH (a) and VRH (b) models. E^a_a and E^{b-c}_a are the activation energies obtained by NNH fitting of the resistivity dependences measured along the *a* axis and within the *b–c* plane, respectively. E^a_{Mott} and E^{b-c}_{Mott} are the Mott hopping energies obtained by VRH fitting of the resistivity dependences measured along the *a* axis and within the *b–c* plane, respectively.

energy, and k_B is the Boltzmann constant. Within the VRH model, we have $\rho_{dc}(T) = \rho_0 \exp[(T_0/T)^{1/4}]$ [16], where ρ_0 is the pre-exponential factor and T_0 relates to the hopping energy as $E_{Mott} = 0.25\ k_B T_0^{1/4} T^{3/4}$. Figure 4 depicts the results of fitting within both models for the data of resistivity measurements within *b–c* plane. A similar result was obtained for the direction within the *a* plane (not presented here).

Using NNH fitting of the resistivity dependences, we estimated the activation energy of small polaron hopping. Contrary to our expectations, E_a for the two different directions in the crystal varies insignificantly: $E^a_a/k_B = 3690$ K and $E^{b-c}_a/k_B = 3600$ K for the directions along the *a* axis and within the *b–c* plane, respectively. However, one can see that the potential barrier to polaron hopping within the MnO_6 layers is lower than that across the layers. Recall that previously [7] we observed the anomaly of heat capacity and irregular change in the lattice parameter near 250 K, where the conductivity character changes. We attributed these features to the cooperative lattice distortion caused by polaron ordering at this temperature. Obviously, this distortion can cause considerable changes in the height of the potential barriers to polaron hopping at temperatures below 250 K, where dielectric relaxation takes place. Hence, the above estimations of the activation energy at $T > 250$ K may not appear quite right for temperatures below 250 K. One may use VRH fitting and estimate the hopping energy of the polarons. At an average temperature of 160 K near which dielectric relaxation is observed, we obtain $E^a_{Mott}/k_B = 2380$ K and $E^{b-c}_{Mott}/k_B = 2245$ K for the directions along the *a* axis and within the *b–c* plane, respectively. One can see that these values are considerably different from the activation energies estimated above within the NNH model. It must be noted, though, that the choice of temperature for the E_{Mott} calculation is arbitrary to a certain extent, so the presented estimates are rather approximate.

Now, we return to the analysis of the dielectric properties. Polaron mobility in ionic crystals, being responsible for conductivity, can also induce dielectric dispersion. Below the temperature of polaron ordering, the ac electric field can induce charge hopping between the equivalent lattice sites available, related to the crystal symmetry. This hopping is equivalent to reorientation of an electric dipole, which yields a frequency-dependent complex dielectric constant with Debye-type behavior. Thus, one may quite reasonably assume that the relaxation-type features in the temperature and frequency dependences of ε' and ε'' are related to hopping of the localized polarons between the specific lattice sites. In order to make quantitative estimations of the characteristic relaxation times and potential barriers determining charge transfer, we applied a generalized Debye model. This model implies a distribution of the relaxation times as compared to the only relaxation time in the conventional Debye theory. In this case, the $\varepsilon'(f)$ and $\varepsilon''(f)$ dependences can be described by the phenomenological Cole–Cole equation with the extra-width parameter α characterizing symmetrical broadening of the Debye relaxation related to the distribution of the relaxation times:

$$\varepsilon = \varepsilon_\infty + \frac{\varepsilon_0 - \varepsilon_\infty}{1 + (i\omega\tau)^{1-\alpha}}. \quad (1)$$

Here ε_0 and ε_∞ are the dielectric constants for the low- and high-frequency limits, respectively, ω is the angular frequency, τ is the characteristic relaxation time. An example of fitting the experimental $\varepsilon'(f)$ and $\varepsilon''(f)$ dependences by the Cole–Cole equations is illustrated in figure 2. Here we show the data for the direction along the *a* axis; a similar procedure was applied to the dependences obtained in the direction within the *b–c* plane. During fitting, we took into account dielectric loss ε''_{dc} related to the conductivity of a sample. The temperature dependences of the relaxation times resulting from the fitting follow well the Arrhenius law $\tau = \tau_0 \exp(E_a/k_B T)$ (figure 5(a)), where E_a is the activation energy, k_B is the Boltzmann constant and τ_0 is the

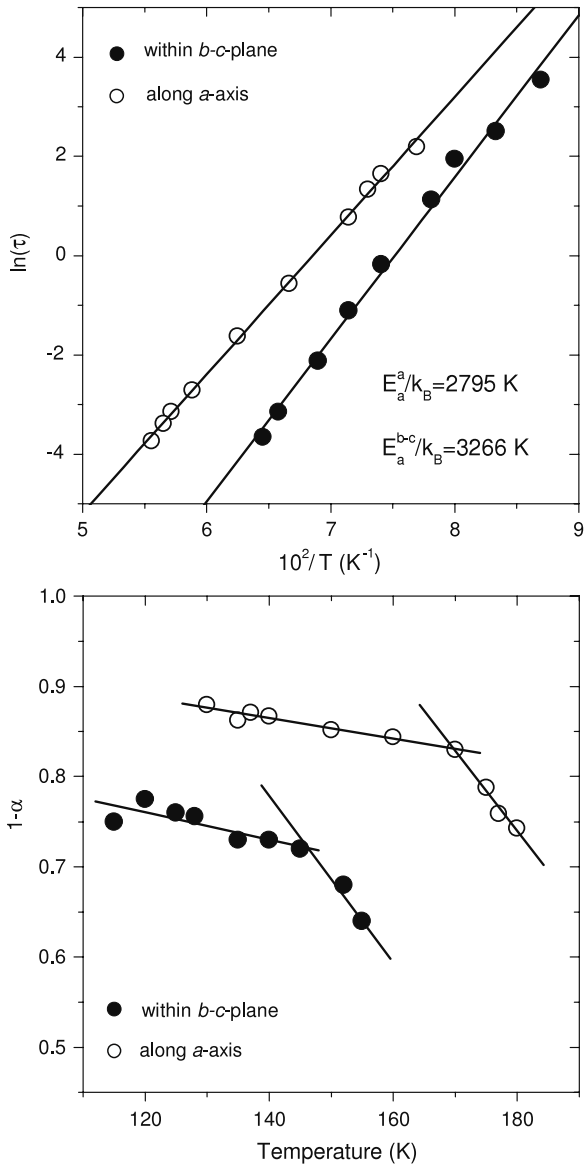

Figure 5. (a) Arrhenius behavior of the relaxation times for the dielectric relaxation process. (b) Temperature variation of the broadening factor (power-law parameter in the Cole–Cole equation) extracted from the data for the two different directions in the crystal: along the a axis and within the b–c plane.

attempt time. The aforesaid evidences a thermally activated mechanism of charge transfer in the crystal; E_a corresponds to the barrier to polaron hopping. Using the fitting procedure, we obtained $E_a^a/k_B = 2795$ K and $E_a^{b-c}/k_B = 3266$ K for the directions along the a axis and within the b–c plane, respectively. These values lie approximately half-way between the activation energy estimations obtained within the NNH and VRH models using the $\rho_{dc}(T)$ data. Surprisingly, the activation energy of polaron hopping within the b–c plane appeared considerably higher than that along the a axis. However, the anisotropy is determined not only by the height of the potential barriers but, to a great extent, by the pre-exponential factor τ_0 characterizing the polaron excitation frequency ($(\tau_0)^{-1}$ is the attempt frequency of jumps) as a result of the interaction with phonon modes in the crystal. In our case, the attempt frequency within the b–c plane ($(\tau_0)^{-1} = 5\times10^{10}$ Hz) is higher by a factor of over 100 than that along the a axis ($(\tau_0)^{-1} = 2 \times 10^8$ Hz). First of all, owing to the anisotropy of the pre-exponential factor, at a fixed temperature the characteristic time of dielectric relaxation is lower by almost an order of magnitude for the direction within the b–c plane than that for the direction along the a axis.

The anisotropy is also revealed in the value of the low-frequency limit of the dielectric constant ε_0. Since this value is determined by a ratio between the charge carrier density n_p and the charge carrier effective mass m_p, $(\varepsilon_0 - \varepsilon_\infty) \propto n_p/m_p$, the analysis of the ε_0 behavior allows us to make definite conclusions concerning the features of the polaron transport in the crystal; ε_0 does not exhibit strong temperature dependence (in the temperature range where the relaxation behavior is observed) for the two selected directions. This is evidence of the invariability of n_p and m_p upon temperature variations. At the same time, it is reasonable to attribute the anisotropy of ε_0 to the anisotropy of the effective polaron mass m_p, as the quantity of the centers participating in polaron motion (a number of equivalent positions in the crystal) should remain invariable.

Regarding the phenomenological parameter α, which characterizes the deviation of the relaxation process from the Debye single relaxation process, it is considered that there may be several reasons increasing this parameter, i.e., broadening the distribution of the relaxation times in the system. First, this parameter is nonzero when the system is characterized by a certain distribution of energy barriers (the barriers to polaron hopping), as often takes place in electronically disordered systems. Second, an increase in α may suggest the development of the correlation between the relaxation units. In this case, polaron hopping is not individual but collective. The correlations between polaron hops result in efficient reduction of the activation energy. Finally, parameter α will be nonzero if the system under study consists of several analogous subsystems with different but close parameters. Such a situation may be implemented, in particular, when there are several nonequivalent positions in the crystal and the polaron hopping processes occur inside each of them along the equivalent sites. One can see in figure 5(b) that in our case the $\alpha(T)$ dependences for the directions within the b–c plane and along the a axis are different. This result is quite expected; the surprise was the presence of sharp kinks at 150 and 170 K in the dependences for the directions within the b–c plane and along the a axis, respectively.

To gain insight into the dielectric relaxation mechanism, one should consider the $Pb_3Mn_7O_{15}$ crystal structure. It is clear from the above arguments that the relaxation process observed in the crystal was attributed to localized polaron hopping between the lattice sites. Note that the chemical formula $Pb_3Mn_7O_{15}$ in itself suggesting the mixed-valence (3+/4+) of manganese ions makes it possible to consider electron hopping between Mn^{3+} and Mn^{4+} as a key mechanism of both dielectric dispersion and conductivity in the crystal. At high temperatures, Mn^{3+} and Mn^{4+} ions randomly occupy the equivalent positions. In the vicinity of 250 K, complete or partial charge ordering occurs, which is evidenced by the

features of the behavior of specific heat, lattice parameter, and conductivity. Below 250 K, the charge motion may be attributed to localized polaron hopping between the lattice sites with a characteristic timescale. When the frequency of the ac electric field coincides with the inverse characteristic relaxation time of the polarons, the real and imaginary parts of dielectric constant exhibit the features typical of the relaxation process discussed above.

Note that charge ordering can occur inside the specific lattice sites related to the same equivalent position. As our last study showed [8], a unit cell of the $Pb_3Mn_7O_{15}$ crystal contains nine nonequivalent positions. The situation can be even more complicated because to date there is no final conclusion about the distribution of the Mn^{3+} and Mn^{4+} ions between the positions. We cannot be sure in which positions the mixed state of the manganese ions is implemented and whether charge ordering occurs in one or several nonequivalent positions. It is not improbable that for different positions the transition to the charge-ordered state will occur at different temperatures: a sufficiently broad transition area may be evidence for this. The relaxation motion of the polarons inside each nonequivalent position will also be characterized by its own set of parameters. Specifically, the activation energy will be determined mainly by a degree of distortion of MnO_6 octahedra; the attempt frequency in the Arrhenius formula, by the interaction with phonon modes in the crystal; and the contribution to the broadening parameter α made by the correlations in polaron motion will be determined, for example, by the ratio between Mn^{3+} and Mn^{4+} within a nonequivalent position.

As far as the anisotropy of the properties is concerned, it is certainly connected with a pronounced layered structure of the crystal. The above estimation shows that the anisotropy is determined not only by the difference in heights of the potential barriers for polaron hopping along different directions in the crystal, but mainly by the attempt frequency. The origin of such a behavior should be searched for in the anisotropy of the phonon spectra of the crystal. Returning to the behavior of parameter α, currently the origin of the observed sharp kinks in the temperature dependences cannot be unambiguously determined with regard to a whole set of the contributions to its value.

4. Conclusions

Having investigated the dielectric properties of the $Pb_3Mn_7O_{15}$ single crystal, we discovered a pronounced feature in the behavior of the real and imaginary parts of the dielectric constant. The character of the frequency and temperature dependences of the dielectric constant allow one to attribute this anomaly to the low-frequency dielectric relaxation process. Study of the crystal structure, the analysis of the results of dielectric measurements using the Debye model, and the data from the resistivity measurements give us grounds to relate the relaxation process to localized polaron hopping between specific lattice sites in the crystals. The anisotropy in the behavior of the dielectric and transport properties is connected with the pronounced crystal anisotropy with the alternating single layers of MnO_6 octahedra and PbO sheets.

Acknowledgments

This study was supported by the Russian Foundation for Basic Research 'Siberia', project No. 09-02-98003, and the Siberian Branch of the Russian Academy of Sciences, integration project No. 101.

References

[1] Eerenstein W, Mathur N D and Scott J F 2006 *Nature* **442** 759
[2] Volkov N V, Sablina K A, Bayukov O A, Eremin E V, Petrakovskii G A, Velikanov D A, Balaev A D, Bovina A F, Böni P and Clementyev E 2008 *J. Phys.: Condens. Matter* **20** 055217
[3] Moore P B, Sen Gupta P K and Le Page Y 1989 *Am. Mineral.* **74** 1186
[4] Seshadri R and Hill N A 2001 *Chem. Mater.* **13** 2892
[5] Chatterji T (ed) 2004 *Colossal Magnetoresistive Manganites* (Dordrecht: Kluwer–Academic)
[6] Ikeda N, Ohsumi H, Ohwada K, Ishii K, Inami T, Kakurai K, Murakami Y, Yoshii K, Mori S, Horibe Y and Kito Y 2005 *Nature* **436** 1136
[7] Volkov N V, Sablina K A, Eremin E V, Böni P, Shah V R, Flerov I N, Kartashev A, Rasch J C E, Boehm M and Schefer J 2008 *J. Phys.: Condens. Matter* **20** 445214
[8] Rasch J C E, Sheptyakov D V, Schefer J, Keller L, Boehm M, Gozzo F, Volkov N V, Sablina K A, Petrakovskii G A, Grimmer H, Conder K and Loffler J F 2009 *J. Solid State Chem.* **182** 1188
[9] Ikeda N, Odaka K, Takahashi E and Kohn K 1997 *Ferroelectrics* **190** 191
[10] Darriet B, Devalette M and Latourrette B 1978 *Acta Crystallogr.* B **34** 3528
[11] Marsh R E and Herbstein F H 1983 *Acta Crystallogr.* B **39** 280
[12] Le Page Y and Calvert L D 1984 *Acta Crystallogr.* C **40** 1787
[13] Li W, Chen K, Yao Y, Zhu J and Wang Y 2004 *Appl. Phys. Lett.* **85** 4717
[14] Freitas R S, Mitchell J F and Schiffer P 2005 *Phys. Rev.* B **72** 144429
[15] Holstein T 1959 *Ann. Phys., NY* **8** 325
[16] Mott N F and Davies E A 1979 *Electronic Processes in Non-Crystalline Materials* (Oxford: Oxford University Press)